Trans. JWRI, Vol. 26 (1997), No. 2

Prediction of Welding Deformation and Residual Stress by Elastic FEM Based on Inherent Strain (Report I)†

- Mechanism of Inherent Strain Production-

Yu LUO*, Hidekazu MURAKAWA** ,Yukio UEDA***

Abstract

The welding residual stress and the distortion are considered to be produced by the inherent strain. The plastic strain in bead welding computed through the Thermal-Elastic-Plastic analysis is an ideal example of the inherent strain, since there is no glove which may introduce additional mismatch. Such inherent strain produced in the welding process is primarily determined by the highest temperature reached and the constraint at each point. Thus, the mechanical phenomena in the bead welding process are closely analyzed by the Thermal-Elastic-Plastic FEM and the mechanism in which the inherent strain is produced is investigated from the aspect of the highest temperature reached and the constraint. Further, based on the knowledge obtained through the study, simple formulae to calculate the inherent strain distribution are proposed. Using the inherent strain given by the formulae, the welding residual stress and the distortion can be predicted by an Elastic FEM analysis.

KEY WORDS: (Inherent strain) (Welding Deformation) (Welding stress) (FEM)

1. Introduction

Along with the development of computer and numerical analysis technology, it becomes possible to simulate the mechanical processes during welding by Thermal-Elastic-Plastic (T.E.P.) FEM[1,2] when the welded structures is simple and small. However, in case of large and complicated welded structures, it is difficult to analyze such non-linear problems because long computing time is required. To ensure the integrity of welded structures, it is necessary to develop a method to investigate welding deformation and residual stress with reasonable computational effort. For this reason, the concept of inherent strain[3-6] has been introduced. Generally, the inherent strain can be considered as a source of both deformations and residual stresses which are produced during thermal processes such as welding, cutting and bending. If the inherent strain for an individual thermal process is known, the deformation and residual stress can be estimated using Elastic FEM in stead of T.E.P. FEM. In this way the computing time can be greatly shortened. Thus, the determination of inherent strain is very important when investigating welding deformation and residual stress in an actual thermal process.

In this paper, the mechanical process in bead welding is simulated by T.E.P. FEM. The computed results clearly show that inherent strain produced in the welding process is primarily determined by the highest temperature reached and the constraint at each point. Thus, the mechanism in which inherent strain is produced is clarified from the aspect of the highest temperature reached and the constraint. Further, based on the knowledge obtained through the study, simple formulae to calculate the inherent strain distribution are proposed. Using the inherent strain given by the formulae, the welding residual stress and the distortion can be predicted by Elastic FEM analysis. The computed results agree well with the available experimental results.

2. Mechanism of inherent strain production

In order to study the mechanism of inherent strain production in welding process, the mechanical behavior of a simple model is investigated first.

† Received on Dec. 5, 1997
* Graduate Student, Osaka University
** Associate Professor
*** Professor, Kinki University

Transactions of JWRI is published by Joining and Welding Reseach Institute of Osaka University, Ibaraki, Osaka 567, Japan.

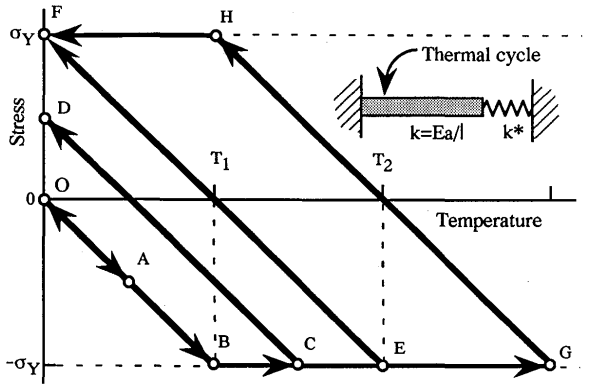

Fig.1 History of stress under thermal cycle for a Bar model with elastic constraint.

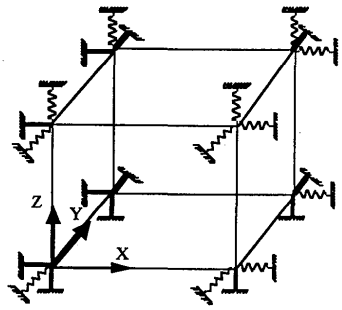

Fig.2 Three dimensional constraint model.

2.1 A bar with elastic constraint

A simple model of a bar with elastic constraint is shown in **Fig.1**. In order to represent the magnitude of the constraint, a parameter β is introduced which is defined as follows,

$$\beta=k^*/(k+k^*) \quad (1)$$

where,

$k=aE/l$	stiffness of bar
k^*	stiffness of spring
a	cross-sectional area of bar
E	Young's modulus of bar
l	length of bar

The relation between the stress and the temperature of the bar during the thermal cycle is shown in **Fig.1**. In the elastic stage, the relation among stress σ, constraint β and temperature T can be expressed as,

$$\sigma=-\beta\alpha TE \quad (2)$$

where, α is the coefficient of linear expansion.

The temperature at which the stress just reaches the yield stress in the heating process is defined as T_1, such that,

$$T_1=\sigma_Y/\beta\alpha E \quad (3)$$

When the bar is constrained completely ($\beta=1$), T_1 is dependent on only material properties and defined as T_Y,

$$T_Y=\sigma_Y/\alpha E \quad (4)$$

If material properties (σ_Y, α, E) are not dependent on temperature, T_Y becomes constant.

Similarly, the heating temperature which is necessary to attain yield stress in the cooling process is defined as T_2, such that,

$$T_2=2T_1 \quad (5)$$

From **Fig.1**, it can be clearly seen that the mechanical behaviors of the bar can be divided into three types according to the highest temperature:

(1) $T_{max}<T_1$

When the highest temperature is lower than T_1 as O-A-O shown in **Fig.1**, the thermal stress at the end of the heating process is smaller than the yield stress. So no inherent strain, deformation nor residual stress is produced.

(2) $T_1<T_{max}<T_2$

When the highest temperature is greater than T_1 but less than T_2, the thermal stress reaches the yield stress in the heating process, and plastic strain is produced. But in the cooling process, additional plastic strain is not produced.

(3) $T_2<T_{max}$

When T_{max} is greater than T_2 as O-B-G-H-F in **Fig.1**, inherent strain is produced in both the heating and the cooling processes.

2.2 A cube with three dimensional elastic constraint

2.2.1 Model of a cube with elastic constraint

In the preceding section, the production mechanism of inherent strain in a thermal cycle for a one dimension model (a bar with elastic constraint) is discussed conceptually. However, the mechanical phenomena in welding processes are not one dimensional. therefore a cube model under three dimensional constraint as shown in **Fig.2** is studied. In this model a cube of size s is constrained by springs which have stiffnesses k^*_x, k^*_y and k^*_z in x, y, z directions, respectively. Similar to the bar model, constraint parameters β_x, β_y and β_z are defined as follows,

$$\beta_i=k^*_i/(k+k^*_i) \quad (i=x, y, z) \quad (6)$$

$k=Es$	stiffness of cube
k^*_i	stiffness of spring in i-th direction
s	size of cube

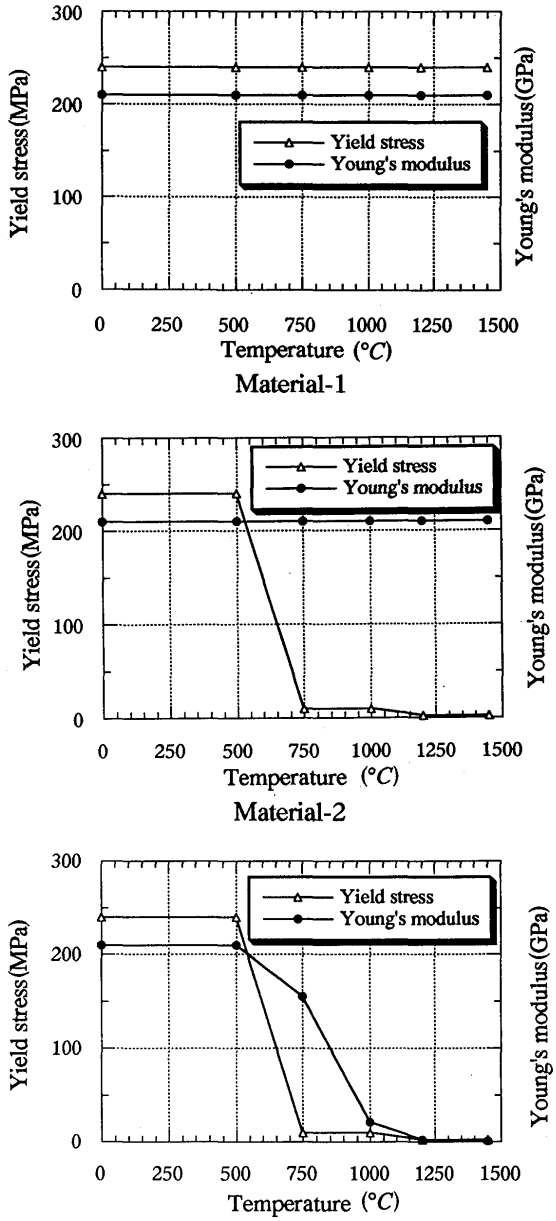

Fig.3 Temperature dependent mechanical properties.

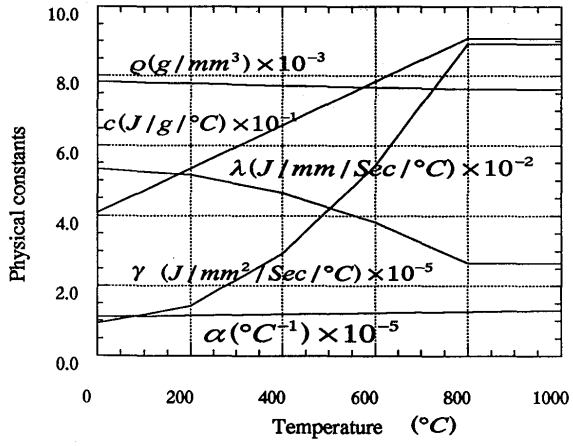

Fig.4 Temperature dependent thermal and physical constants.

Fig. 3 shows the relation between the temperature and the yield stress and Young's modulus used in this study. Three kinds of materials are considered. Material-3 is close to actual mild steel. Both yield stress and Young's modulus are dependent on temperature. In the case of material-2, only yield stress is dependent on temperature. In the case of material-1, neither yield stress nor Young's modulus is dependent on temperature. The thermal and physical constants used are shown in **Fig.4**. The constraint parameter β_X, β_Y, β_Z was determined with reference to material properties at room temperature.

To clarify the mechanism of inherent strain production under three dimensional constraint, a series of computations are made using Thermal Elastic Plastic (T.E.P.) FEM.

2.2.2 Relation between highest temperature and residual stress

Corresponding to the welding model discussed in this report, x, y and z directions refer to the welding, the transverse and the thickness directions, respectively. In general, the constraint is the strongest in the welding direction and that in the thickness direction is the weakest. **Fig. 5** shows the relation between the highest temperature and the residual stress which is obtained as computed results for material-1 when $\beta_Y=\beta_Z=0$. From this figure, it is clearly seen that the mechanical behavior of the cube is the same as that of the bar model since the constraints in y and z directions β_Y, β_Z are zero. Thus, when $T<T_{1X}$, no residual stress is produced. When $T_{1X}<T<T_{2X}$, the residual stress increases with the temperature. When $T>T_{2X}$, the residual stress becomes equal to the yield stress independent of temperature, where,

$T_{1X}=\sigma_Y/\beta_X\alpha E$, $\quad T_{2X}=2T_{1X}$

On the other hand, T_{1X} increases with the decrease of β_X. It is only when $T_{1X}<T_{max}<T_{2X}$ that β_X influences the value of the residual stress.

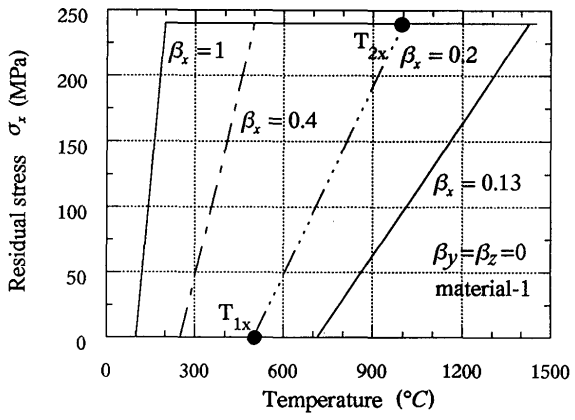

Fig.5 Relation between residual stress and maximum temperature.

2.2.3 *Influence of highest temperature and constraint on inherent strain*

The relation among the constraint, the highest temperature and the inherent strain is given in **Fig.6**. The conditions for the analysis in **Fig.6(a)** are the same as those in the preceding section. For the computation in **Fig.6(b)**, $\beta_y=1$ is assumed to represent the effect of the constraint in transverse direction. From **Fig.6** it is seen that the curve can be divided into three regions according to β_x, such that,

$$\varepsilon^*_x=0 \qquad T_{1x}>T_{max} \qquad (7)$$
$$\varepsilon^*_x=-\alpha T_{max}+\varepsilon_Y/\beta_x \qquad T_{1x}<T_{max}<T_{2x}$$
$$\varepsilon^*_x=-\varepsilon_Y/\beta_x \qquad T_{max}>T_{2x}$$

where,

$\varepsilon_Y=\sigma_Y/E$

$T_{1x}=\sigma_Y/\beta_x\alpha E$

$T_{2x}=2\sigma_Y/\beta_x\alpha E$

As described by the above formulas, the inherent strain ε^*_x is influenced by the highest temperature T_{max} only when $T_{1x}<T_{max}<T_{2x}$.

Comparing **Fig.6(a)** and **Fig.6(b)**, it is found that the curve is basically similar, especially when $0.2<\beta_x<0.8$. In the welding process, the constraint parameter in the welding direction is about in this range. Thus, the inherent strain in the welding direction is mainly determined by the constraint parameter, β_x. Influence from the constraint in the transverse direction β_y is small.

It is also seen that, the inherent strain has a peak value at certain value of β_x. If constraint is larger or smaller than this peak, the absolute value of inherent strain decreases. Since $\beta_x\approx1$ in the welding direction, the inherent strain is nearly equal to the yield strain. On the other hand, constraint in the transverse direction β_y is very small. Thus, the inherent strain ε^*_y is large and dependent on both the constraint and the highest temperature.

Assuming that $\beta_y=0.01$, $\beta_z=0$ and considering material-3, which is closer to actual steel, serial computations are made. The relations between the inherent strain ε^*_x, ε^*_y and the highest temperature are shown in **Fig.7** and **Fig.8**, respectively. It is seen from **Fig.7** that ε^*_x is independent of temperature and determined by β_x when the temperature is higher than T_{2x}. It is also clearly seen from **Fig.8** that ε^*_y is dependent on temperature and not influenced by β_x. When the highest temperature is lower than the mechanical

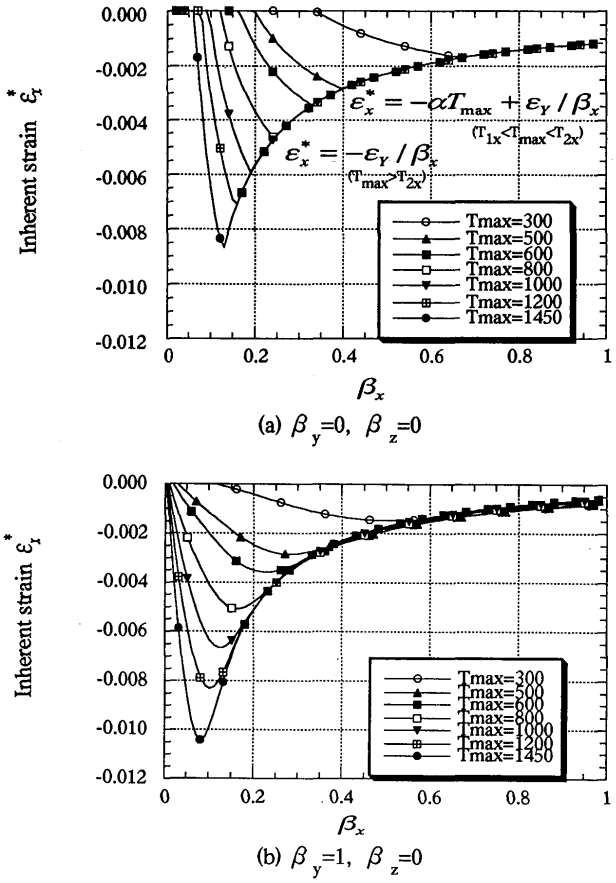

Fig.6 Effect of maximum temperature and constraint on inherent strain in welding direction.

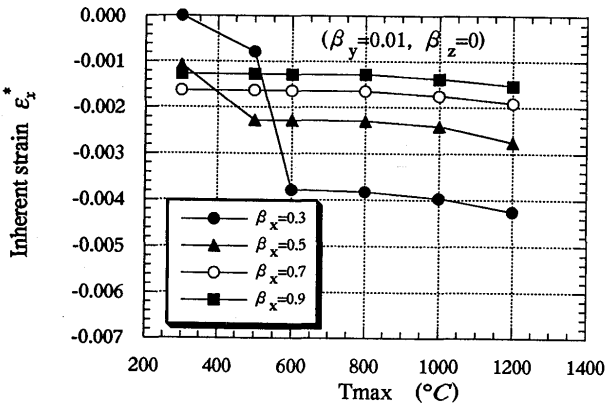

Fig.7 Relation between maximum temperature and inherent strain in welding direction.

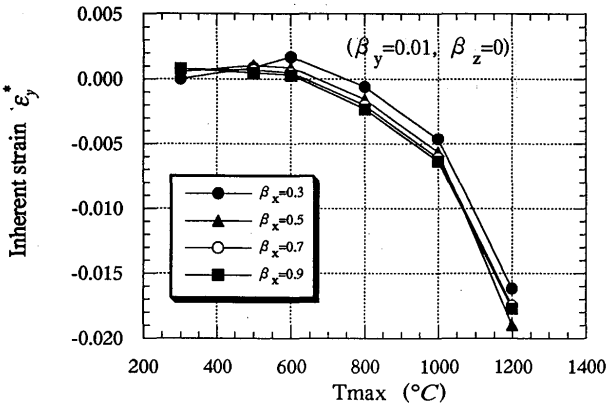

Fig.8 Relation between maximum temperature and inherent strain in transverse direction.

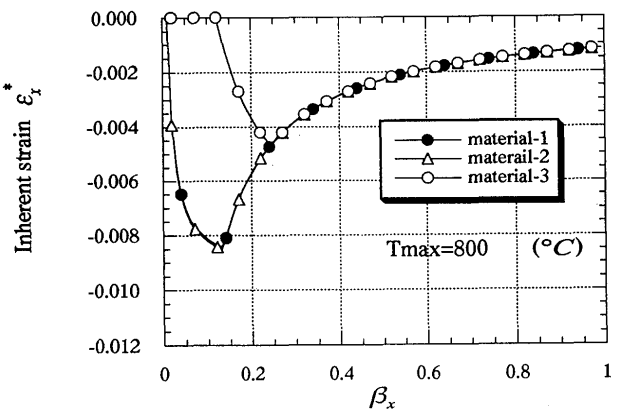

Fig.9 Relation between β_X and ε_X^* for three materials at 800℃.

melting point, ε^*_y is nearly equal to zero and it increases with the temperature when the temperature is high.

2.2.4 Influence of material properties

Fig. 9 shows the relation between β_X and ε^*_X for three different materials when the highest temperature is 800°C. From **Fig.9**, it is concluded that the inherent strain is not influenced by material properties when the constraint is strong (in this case β_X>0.25). But when the constraint is very small, the inherent strain is strongly dependent on material properties.

3. Computation of welding deformation and residual stress

3.1 Model for analysis

As shown in **Fig.10**, a bead weld was applied on a plate of width: 400mm, length: 200 mm and thickness: 16 mm. Four cases of heat input are assumed as follows,

case(1): Q=533J/mm, (Q*=5.0)

case(2): Q=800J/mm, (Q*=7.5)

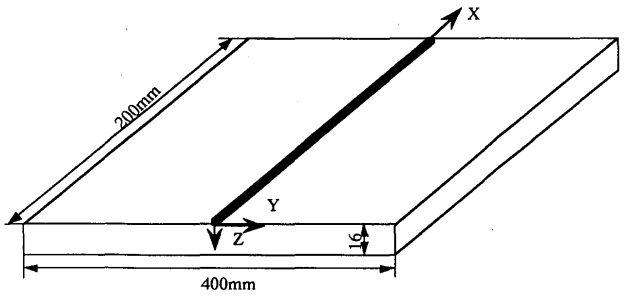

Fig.10 Bead welding model.

case(3): Q=1067J/mm, (Q*=10.0)

case(4): Q=1333J/mm, (Q*=12.5)

Q* is the dimensionless heat input per unit length defined by,

$Q^*=Q/h^2c\varrho T_Y$

where h, c and ϱ are the thickness, the thermal capacity and the density, respectively. T_Y is given by Eq. (4). The welding speed is 4.3mm/sec. The mechanical properties are given in **Fig.3**(material-3) and the physical properties defined in **Fig.4** are used. The bead welding is simulated using both the plane strain model and the three dimensional model.

3.2 Plane strain model

3.2.1 Examination of inherent strain in plane strain model

To examine the inherent strain in bead welding, the T.E.P. FEM is used. The distribution of the highest temperature and the inherent strains on the surface for case(2) are shown in **Figs.11(a)** and **(b)**. From these figures, the features of inherent strain can be described as follow.

(1) for ε^*_X

$T_{max}<T_{1x}$

$\varepsilon^*_X=0$ (no plastic strain)

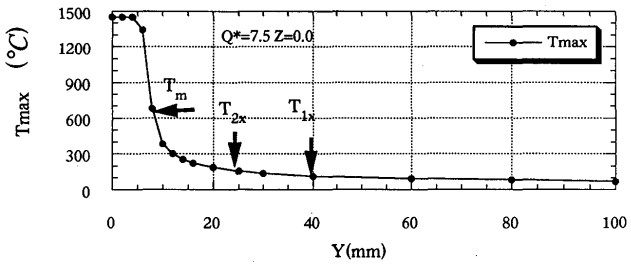

(a) Distribution of temperature

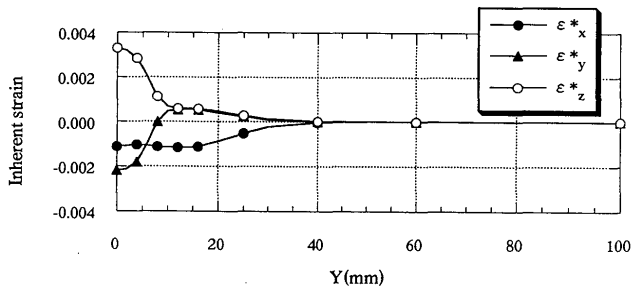

(b) Distribution of inherent strain

Fig.11 Distribution of temperature and inherent strains in transverse direction.

$T_{1x}<T_{max}<T_{2x}$

ε^*_x (increases with T_{max})

$T_{2x}<T_{max}$

$\varepsilon^*_x=-\varepsilon_Y/\beta_x$ (for plane strain $\beta_x=1$)

$=-\sigma_Y/E=0.00114$

where, $T_{1x}=-\sigma_y/E\beta_x\approx100°C$

(2) for ε^*_y

$T_{max}<T_{1x}$

$\varepsilon^*_y=0$ (no plastic strain)

$T_{1x}<T_{max}<T_m$

$\varepsilon^*_y=\varepsilon^*_z$ (because $\beta_y\approx\beta_z<<\beta_x$)

$T_m<T_{max}$

ε^*_y (increases with T_{max})

where, T_m is the mechanical melting point.

(3) for ε^*_z

$\varepsilon^*_z=-(\varepsilon^*_x+\varepsilon^*_y)$ (incompressibility)

3.2.2 *Formulae of inherent strain for plane strain model*

As explained in the preceding section, the main factors which influence the inherent strain are the highest temperature and the constraint. Simple formulae to calculate the inherent strain, which is a function of the highest temperature and the constraint, are proposed as follows for the plane strain model.

for inherent strain in welding direction

$\varepsilon^*_x=0$ $T_{max}<T_{1x}$

$\varepsilon^*_x=-\alpha(T_{max}-T_{1x})$ $T_{1x}<T_{max}<T_{2x}$

$\varepsilon^*_x=-\varepsilon_y$ $T_{2x}<T_{max}$ (8)

for inherent strain in transverse direction

$\varepsilon^*_y=0$ $T_{max}<T_{1x}$

$\varepsilon^*_y=\varepsilon^*_z=-\varepsilon^*_x/2$ $T_{1x}<T_{max}<T_m$

(incompressibility)

$\varepsilon^*_y=-A\alpha(T_{max}-T_m)+\varepsilon_Y/2$ $T_m<T_{max}$ (9)

To derive Eq.(9), it is assumed that ε^*_y is a linear function of T_{max} in this region as observed in **Fig.7**. Also, the continuity condition of the inherent strain ε^*_y at $T_{max}=T_m$ is assumed, i.e..

$\varepsilon^*_y=\varepsilon_Y/2$.

for inherent strain in thickness direction

$\varepsilon^*_z=-(\varepsilon^*_x+\varepsilon^*_y)$ (incompressibility) (10)

for shear inherent strain

According to the symmetry, the shear inherent strain is assumed to be an odd function of y. Considering the results of T.E.P. FEM, the distribution of the shear inherent strain is represented by the following equation.

$\gamma^*_{yz}=B\alpha(T_{max}-T_{2x})(y/h)$ (11)

where, the material properties at room temperature are given as,

$\sigma_Y=240$ MPa

$\alpha=1.14\times10^{-5}$ °C^{-1}

E=210 GPa

$T_{1x}=100$ °C

$T_{2x}=200$ °C

$T_m=750$ °C

h: thickness of plate

The unknown coefficients in the above formulae are A and B. These can be determined by T.E.P. FEM or by experiment. For example, from the results computed by T.E.P. FEM for the four cases, it is found that,

$T_{max}=1450$ °C, $\varepsilon^*_y\approx-0.00225$ at y=0, z=0

By substituting this condition into Eq.(9), it is found that,

A=0.35

Also from the computed results by T.E.P. FEM, the constant B is determined to be,

B=1.7

3.2.3 *Comparison of results by T.E.P. FEM and Elastic FEM's*

Using the inherent strain, the deformations and the residual stresses caused by a bead welding are computed by Elastic FEM. The inherent strain is calculated using the proposed formulae and the highest temperature to be used is computed by FEM. The highest temperature can be also estimated using appropriate analytical solutions. **Figs. 12, 13** show the distribution of inherent strains for case(2) obtained from the T.E.P. FEM and that

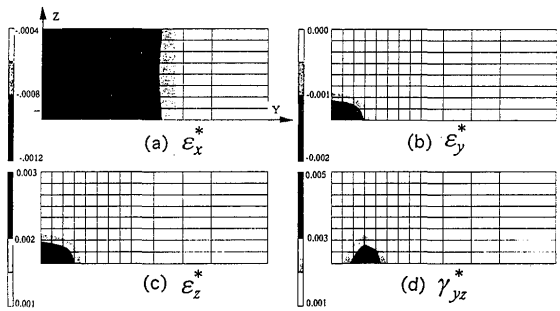

Fig.12 Distribution of inherent strain by thermal-elastic-plastic-analysis (case(2)).

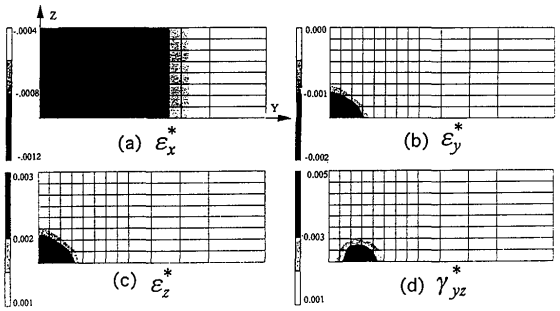

Fig.13 Distribution of inherent strain computed by proposed formula (case(2)).

calculated using the proposed formulae, respectively. The distributions of residual stresses computed by the T.E.P. and the Elastic FEM's are shown in **Figs.14 and 15.** Similarly, the comparison between angular distortions is shown in **Fig.16.** From these figures, it is seen that the deformation and the residual stresses can be predicted with reasonable accuracy by Elastic FEM using the inherent strain.

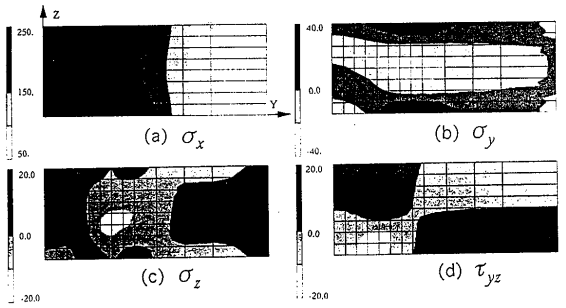

Fig.14 Stress distribution computed by thermal-elastic-plastic analysis (case(2)).

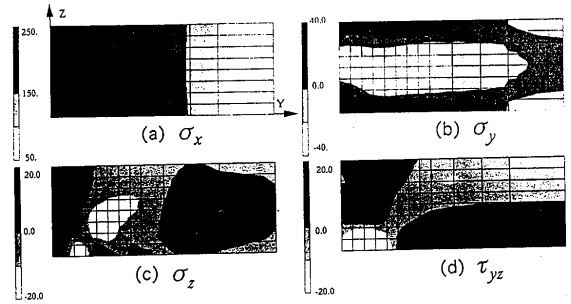

Fig.15 Stress distribution computed by elastic FEM using inherent strains (case(2)).

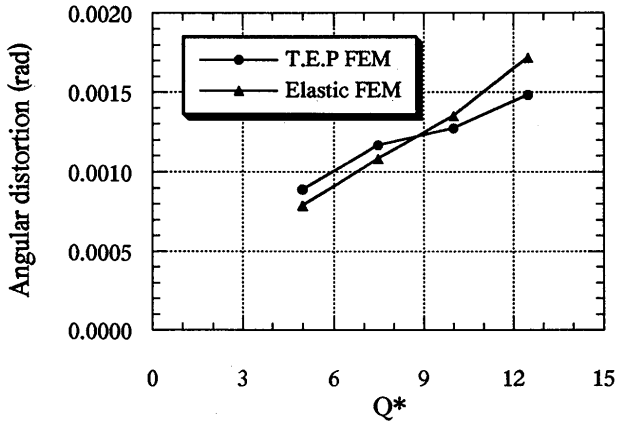

Fig.16 Comparison between angular distortion computed thermal-elastic analysis and proposed elastic analysis.

3.3 3-D model for bead welding with moving heating source

3.3.1 Feature of inherent strain in the 3-D model

The 3-D model is different from the plane strain model mainly in constraint. In case of plane the strain model, deformation in the welding direction is fully constrained, whereas that in the transverse direction is nearly free, i.e..

$\beta_x=1$ $\beta_y \approx \beta_z \approx 0.0$

In case of the 3-D model, the constraint in the welding direction is smaller than that in the plane strain model, but it is larger in the transverse direction.

The distribution of the highest temperature and the inherent strains on the surface at the middle transverse section in case(2) are shown in **Figs.17(a)** and **(b).** From these figures, the following features of the inherent strain are observed.

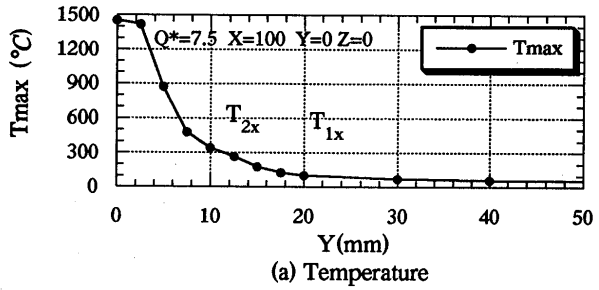

(a) Temperature

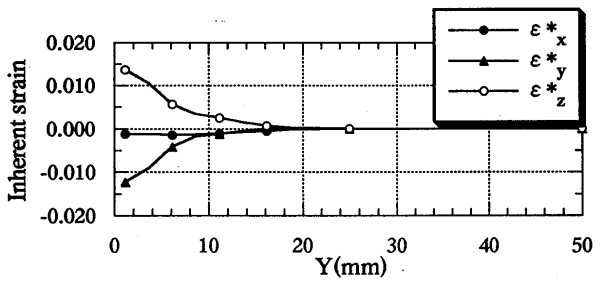

(b) Thermal-elastic-plastic FEM

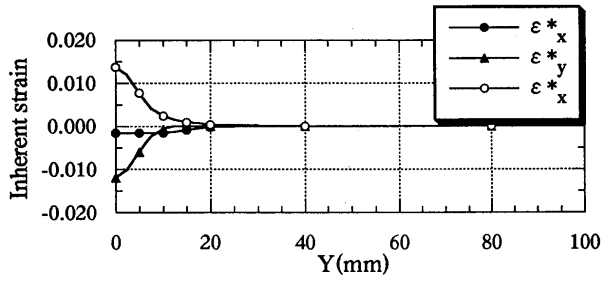

(c) Proposed formula

Fig.17 Distribution of temperature and inherent strain by thermal-elastic-plastic analysis and proposed formula (case(2)).

(1) for ε^*_x

$T_{max}<T_{1x}$

$\varepsilon^*_x=0$ (no plastic strain)

$T_{1x}<T_{max}<T_{2x}$

ε^*_x (increases with T_{max})

$T_{2x}<T_{max}$

$\varepsilon^*_x=-\varepsilon_Y/\beta_x$ ($0<\beta_x<1$)

where, $T_{1x}=-\sigma_Y/E\beta_x$, $T_{2x}=2T_{1x}$

(2) for ε^*_y

$T_{max}<T_{2x}$

$\varepsilon^*_y=0$ (because $\beta_y<\beta_x$, $T_{1y}\geq T_{2x}$)

$T_{2x}<T_{max}$

ε^*_y (increases with T_{max})

(3) for ε^*_z

$\varepsilon^*_z=-(\varepsilon^*_x+\varepsilon^*_y)$ (incompressibility)

3.3.2 *Formulae of inherent strain for the 3-D model*

The shear components of the inherent strain γ_{xy},γ_{zx} are assumed to be negligible. Simple formulae which determine the inherent strain in the 3-D model as functions of the highest temperature and the constraint are given as,

when $T_{max}<T_{1x}$

$$\varepsilon^*_x=\varepsilon^*_y=\varepsilon^*_z=\gamma_{xy}=\gamma_{zx}=\gamma_{yz}=0 \quad (12)$$

when $T_{1x}<T_{max}<T_{2x}$

$$\varepsilon^*_x=-\alpha T_{max}+\varepsilon_Y/\beta_x \quad (13)$$
$$\varepsilon^*_y=0$$
$$\varepsilon^*_z=-(\varepsilon^*_x+\varepsilon^*_y)$$
$$\gamma_{yz}=0$$

when $T_{2x}<T_{max}$

$$\varepsilon^*_x=-\varepsilon_Y/\beta_x$$
$$\varepsilon^*_y=-A\alpha(T_{max}-C)$$
$$\varepsilon^*_z=-(\varepsilon^*_x+\varepsilon^*_y)$$
$$\gamma^*_{yz}=B\alpha(T_{max}-T_{2x})(y/h) \quad (14)$$

The unknown coefficients in the above formulas are A, B, C and β_x.

In case of the 3-D model, β_x depends on heat input Q*. From the definition, β_x and T_{1x} can be related through the following equation.

$$T1x=\sigma Y/E\alpha\beta x \quad (15)$$

T_{1x} can be considered as the temperature at which ε^*_x just begins to be produced. From the results of T.E.P. FEM for the four cases, the relation between T_{1x} and Q* is obtained as follows.

$$T_{1x}=100+5Q^* \quad (16)$$

By comparing Eqs.(15) and (16), the following equation is derived.

$$\beta_x=1/(1+0.05Q^*) \quad (17)$$

The constant C can be decided by considering the continuity condition of ε^*_y at $T_{max}=T_{2x}$ in Eq.(14), i.e..

$$\varepsilon^*_y(T_{2x})=0$$

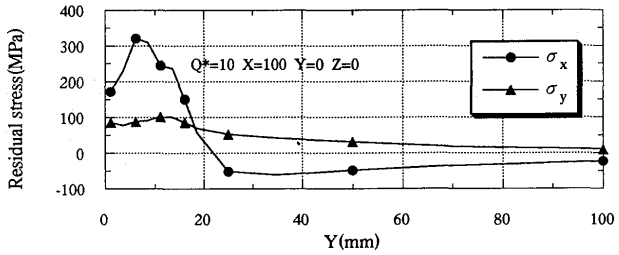

(a) Thermal-elastic-plastic FEM

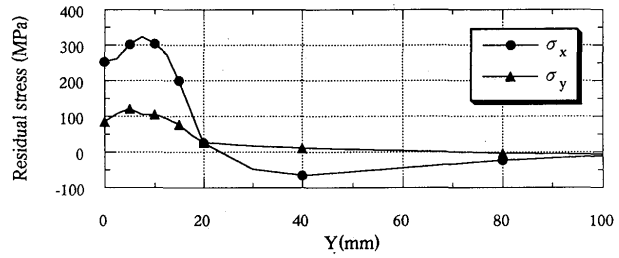

(b) Elastic FEM using inherent strain

Fig.18 Comparison between stresses computed by thermal-elastic-plastic and proposed elastic analysis (case(3)).

From the above condition, it is found that,

$$C=T_{2x}$$

According to the results of T.E.P. FEM, the relation between Q* and ε^*_y in the middle of the welding line (x=100, y=0, z=0, T_{max}=1450°C) can be approximated as a linear function, i.e..

$$\varepsilon^*_y=-0.0035(1+0.4Q^*) \quad (18)$$

By comparing Eqs.(18) and (14) , the constant A is determined to be,

$$A\approx 0.26(1+0.4Q)$$

Similarly, based on the results computed by T.E.P. FEM, B can be determined, i.e..

$$B\approx 3.6+1.28Q^* \quad (19)$$

3.3.3 *Comparison between results by T.E.P. and Elastic FEM's*

The distribution of inherent strains on the surface of the middle transverse section for case(2) calculated by the proposed formulae is shown in **Fig.17(c)**. **Fig. 18** shows the comparison between the residual stresses in case(3) computed by the T.E.P. and the Elastic FEM's. The transverse shrinkage and the angular distortion computed by the FEM's are compared with the values measured by Satoh et. al[7] in **Figs.19** and **20**, respectively. As seen from these comparisons, the elastic FEM using inherent strain determined by the proposed formulae can be used to predict welding residual stresses and distortions with an acceptable accuracy.

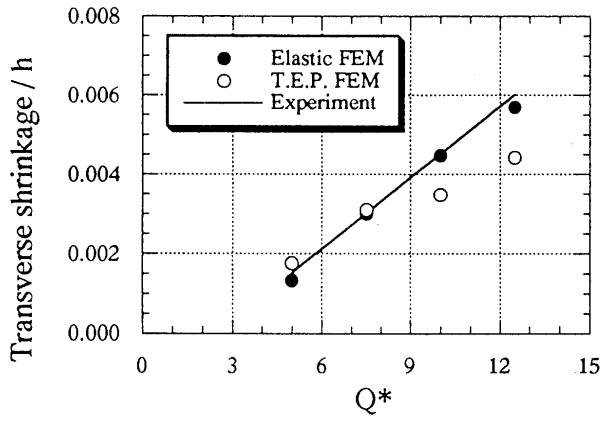

Fig.19 Comparison between transverse shrinkage computed by thermal-elastic-plastic and proposed elastic analysis.

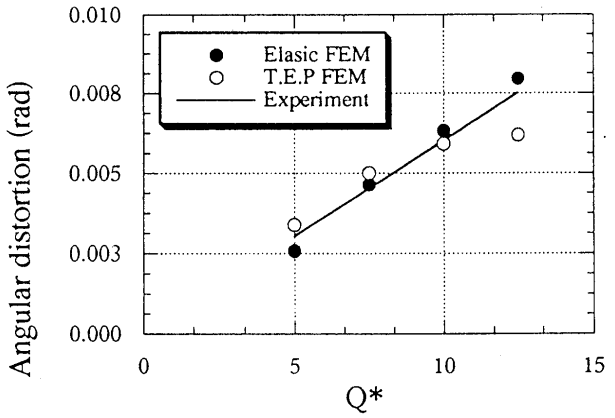

Fig.20 Comparison between angular distortion computed by thermal-elastic-plastic and proposed elastic analysis.

4. Conclusions

The main conclusions drawn from the present study are summarized as follows:

(1) It is reasonable to consider that the residual stress and the distortions in bead welding are produced by the inherent strain.

(2) The inherent strain produced in the bead welding process is primarily determined by the highest temperature reached and the constraint at each point. The mechanism by which the inherent strain is produced is examined from these aspects.

(3) Simple formulae to calculate the inherent strain distribution are proposed. Using the inherent strain given by the formulae, the welding residual stress and the distortion can be predict by elastic FEM analysis.

(4) The residual stresses and distortions predicted by Elastic FEM using proposed inherent strain formulae agree well with those computed by T.E.P. FEM, and also with reported experimental measurements.

References

1) Y. Ueda and T. Yamakawa, "Analysis of Thermal Elastic-Plastic Stress and Strain during Welding", IIW Doc. X-616-71(1971), also Trans. Japan Welding Soc., Vol.2 (1971), No.2, 90-100.

2) Y. Ueda, H. Murakawa, S. M. Gu, Y. Okumoto and M. Ishiyama, "Simulation of Welding Deformation for Accurate Ship Assembling (Report III) - Out-of-plane Deformation of Butt Welded Plate -", Trans. Soc. Naval Architects of Japan, No.176 (1994), 341-350 (in Japanese).

3) M. Masubuchi, "Stress due to the Distributed Incompatibility", Trans. Soc. Naval Architects of Japan, No.88 (1955), 189-200 (in Japanese).

4) Tsugio Fujimoto, "A method for analysis of residual welding stresses and deformations based on the inherent strain", Japan Welding Soc., Vol.39-4 (1970), 236-252 (in Japanese).

5) Y. Ueda and M. G. Yuan, "A Predicting Method of Welding Residual Stress Using Source of Residual Stress (Report III)", Trans. JWRI, Vol.22 (1993), No.1, 157-168, also Trans. ASME, J. Eng. Materials and Technology, Vol.115 (1993), 417-423.

6) Y. Ueda, N. X. Ma, Y. S. Wang and R. Koki, "Measurement of Residual Stresses in Single-pass and Multipass Fillet Welds Using Inherent Strains -Estimation and Measuring Methods of Residual Stresses Using Inherent Strain Distribution Described as Functions (Report V)", Quarterly J. Japan Welding Soc., Vol.13 (1995), No.3, 470-478.

7) K.Satoh and T. Terasaki, " Effect of Welding Conditions on Welding Deformations in Welded Structural Materials", Journal of the Japan Welding Society, Vol.45, No.4(1976), pp.302-308(in Japanese).